Comparison of theoretical models of crossover behavior near the ^{3}He liquid-vapor critical point

Fang Zhong and M. Barmatz
Jet Propulsion Laboratory, California Institute of Technology, Pasadena, California 91109-8099, USA
(Received 18 August 2004; published 2 December 2004)

Parametric expressions, based on three different theoretical models, are used to calculate the isothermal susceptibility, specific heat, and order parameter along the critical isochore and coexistence curve from the asymptotic region to the crossover region. These models are (i) the minimal-subtraction renormalization scheme, (ii) the massive renormalization scheme within the ϕ^4 model, and (iii) the crossover parametric model based on the crossover Landau model. We fit these theories globally to experimental measurements of the isothermal susceptibility and specific heat along the critical isochore and coexistence curve, and to the coexistence curve of ^{3}He near its liquid-vapor critical point. All of the theories provide good agreement with the experimental measurements within the reduced temperature range $|t| \leqslant 2\times 10^{-2}$. The differences in the fits between the theories and the correlations between the adjustable model parameters are discussed.

DOI: 10.1103/PhysRevE.70.066105 PACS number(s): 64.60.Ak, 05.10.Cc, 05.70.Jk

I. INTRODUCTION

It is well known that many thermodynamic quantities exhibit singularities asymptotically close to the critical point. The power-law behavior of these singularities, characterized by critical exponents and the concept of universality and scaling, has been successfully described by renormalization-group (RG) theory [1]. Away from the asymptotic region, thermodynamic quantities of real physical systems deviate from simple power-law behavior. However, RG theory can still provide insight in understanding behavior in this crossover region.

There are two main field-theoretical renormalization-group schemes that treat critical-to-classical crossover phenomena. Dohm and co-workers developed the minimal-subtraction renormalization (MSR) scheme [2–5] while Bagnuls and Bervillier developed the massive renormalization (MR) scheme [6,7]. Both of these theories used the Borel resummation technique to describe crossover behavior within the ϕ^4 model in any $O(n)$ universality class and in three dimensions. The differences between the two schemes were discussed in Ref. [4]. These field-theoretical crossover theories were improved over the years as asymptotic theories became more accurate [8]. Recently, Larin *et al.* improved the MSR expressions for the specific heat and compared their results with the superfluid helium $(n=2)$ system [9]. Bagnuls and Bervillier have also improved their theory to match the more recent asymptotic values for exponents and leading amplitude ratios [10–12]. Both renormalization schemes can provide crossover functional forms for thermal properties with a minimal set of fluid-dependent adjustable parameters. However, these two renormalization schemes only apply to the primary critical paths (critical isochore and coexistence curve) and are not as yet models for a complete equation of state. Recently, Agayan *et al.* developed a phenomenological crossover parametric model (CPM) equation of state [13] that is also consistent with RG theory. The internal constants within this model were adjusted such that the ratios of asymptotic and first correction-to-scaling amplitudes agreed to within theoretical uncertainties with the values determined in renormalization-group theory [13].

Traditionally the susceptibility χ_T, specific heat C_V, and coexistence curve $\Delta\rho_{L,V}$ can be expressed in terms of the standard Wegner expansion as

$$\chi_T^{\pm} = \Gamma_0^{\pm}|t|^{-\gamma}(1+\Gamma_1^{\pm}|t|^{\Delta}+\cdots), \tag{1}$$

$$C_V^{\pm} = A_0^{\pm}|t|^{-\alpha}(1+A_1^{\pm}|t|^{\Delta}+\cdots)+B_{\mathrm{cr}}+C_B, \tag{2}$$

$$\Delta\rho_{L,V} = \pm B_0|t|^{\beta}(1+B_1|t|^{\Delta}+\cdots). \tag{3}$$

Here $t\equiv T/T_c-1$ is the reduced temperature with T_c being the critical temperature. α, β, γ, and Δ are universal critical exponents whose values are estimated from RG theory. For susceptibility, "+" is along the critical isochore above T_c, and "−" is along the coexistence curve below T_c. For specific heat, "+" is along the critical isochore above T_c, and "−" is along the critical isochore in the coexisting phases below T_c, and B_{cr} and C_B are the critical and analytical background contributions, respectively. For the coexistence curve, "+" and "−" stand for the liquid and vapor phases respectively. $\Gamma_0^{\pm}$, $A_0^{\pm}$, and B_0 are the leading asymptotic critical amplitudes and $\Gamma_1^{\pm}$, $A_1^{\pm}$, and B_1 are the first Wegner expansion amplitudes. All the critical amplitudes in Eqs. (1)–(3) can be expressed in terms of fluid-dependent model parameters as well as the values of model-independent universal parameters. In this paper we will present a direct comparison of the three theoretical models to various experimental measurements near the liquid-gas critical point of ^{3}He.

II. FIT TO EXPERIMENTAL MEASUREMENTS

In fitting experimental measurements y_{expt} to theory, we minimize

$$\chi^2 = \sum_{i=1}^{N}\left(\frac{y_{\mathrm{expt},i}-y_{\mathrm{theory}}(x_i,\vec{a})}{\sigma_i}\right)^2, \tag{4}$$

where $\vec{a}$ is an array of fitting parameters, x_i is an independent variable (reduced temperature or temperature in our case), and σ_i is the standard error assigned to each experimental

measurement. The goodness of a fit is characterized by the value

$$\chi_\nu^2 = \frac{\chi^2}{N-M}, \tag{5}$$

where N is the number of data points and M is the number of fitting parameters.

In this paper, we perform a joint fit of the three thermal properties, isothermal susceptibility, specific heat, and coexistence curve, in order to more completely test the theoretical models than fitting the properties separately. To make sure that no particular measurement dominates the joint fit, a proper weighting is needed to balance the varying numbers of measurements in different properties. We chose the following weighting in order to normalize an average $\overline{\chi^2}$ by the number of data points:

$$\overline{\chi^2} = \frac{N}{3}\left(\frac{\chi_{\chi_T}^2}{N_{\chi_T}} + \frac{\chi_{C_V}^2}{N_{C_V}} + \frac{\chi_{\Delta\rho_{L,V}}^2}{N_{\Delta\rho_{L,V}}}\right) \tag{6}$$

where $N=N_{\chi_T}+N_{C_V}+N_{\Delta\rho_{L,V}}$ is the total number of data points.

The standard error σ for each index i in Eq. (4) is given by

$$\sigma^2 = \sigma_y^2 + \left(\frac{\partial y}{\partial x}\right)_{\vec{a}}^2 \sigma_x^2. \tag{7}$$

The partial derivative in Eq. (7) is evaluated numerically in each fitting iteration. We assumed each measurement has a k% uncertainty and assigned $\sigma_y = k \times y/100$. Based on the measurement uncertainties reported in Ref. [14], we assigned the uncertainties in the measured susceptibility to be $\sigma_{\chi_T}(T>T_c)=0.02\chi_T(T>T_c)$ and $\sigma_{\chi_T}(T<T_c)=0.1\chi_T(T<T_c)$. The uncertainties in the measured specific heat were assigned to be $\sigma_{C_V}(T>T_c)=0.01C_V(T>T_c)$ and $\sigma_{C_V}(T<T_c)=0.05C_V(T<T_c)$. The uncertainties in the measured coexistence curve were assigned to vary monotonically from 1% at $|t|=6\times10^{-4}$ to 0.2% at $|t|=1\times10^{-2}$. In the joint fit, χ_T and C_V were fitted against temperature T while $|\Delta\rho_{L,V}|$ was fitted against reduced temperature $|t|$. The uncertainty in the temperature measurement for χ_T and C_V was assigned to be $\sigma_x = 1\times10^{-5}$ K which corresponded to an uncertainty for any reduced temperature of $\sigma_x/T_c = 3\times10^{-6}$ K.

All the experimentally measured quantities were made dimensionless by expressing them in units of appropriate combinations of the ^{3}He critical temperature $T_c=3.315$ K, critical density $\rho_c=0.041\,45$ g/cm^3, and critical pressure $P_c=0.1146$ MPa.

In fitting specific heat data to theoretical models, the analytical background C_B was taken to be an adjustable parameter. The true crossover behavior described by the models can be revealed when C_B is considered a constant within a small reduced temperature range around T_c. To this end, the fits were limited to the reduced temperature range $|t|\leqslant 2\times10^{-2}$. In fitting coexistence curve data to theoretical models, a background contribution, resulting from order parameter saturation and only important further away from the critical point [14], was not included. Therefore, the coexistence curve fit was limited to the reduced temperature range $|t|\leqslant 4\times10^{-2}$.

III. THEORETICAL EXPRESSIONS OF MINIMAL-SUBTRACTION RENORMALIZATION SCHEME

Detailed derivations of theoretical expressions based on the minimal-subtraction renormalization scheme were given in a previous publication [14]. References to the original studies by Dohm and co-workers were also given in Ref. [14]. In this paper, we summarize the key expressions. The Hamiltonian for the ϕ^4 model in three dimensions ($d=3$) is

$$H_\phi = \int d^3x \left\{ \frac{1}{2} r_0 \phi_0^2 + \frac{1}{2} (\nabla \phi_0)^2 + u_0 \phi_0^4 \right\}, \tag{8}$$

where ϕ_0 is the order parameter field. The nonuniversal parameter u_0 is the fourth-order coupling constant and the parameter r_0 is related to the reduced temperature by

$$r_0 - r_{0c} = a_0 t, \tag{9}$$

where a_0 is a nonuniversal constant and r_{0c} is the value of r_0 at the critical point. The total Hamiltonian is the sum $H=H_\phi+H_0$, where H_0 is the analytic background free energy.

The dimensionless bare order parameter field ϕ_0 and the bare coupling parameters u_0 and r_0 are renormalized to ϕ, u, and r by the expressions

$$\phi = Z_\phi(u,\epsilon)^{-1/2}\phi_0, \tag{10}$$

$$u = \mu^{-1} Z_u(u,\epsilon)^{-1} Z_\phi(u,\epsilon)^2 A_3 u_0, \tag{11}$$

$$r = Z_r(u,\epsilon)^{-1}(r_0 - r_{0c}), \tag{12}$$

where μ^{-1} is an arbitrary reference length, $A_3=(4\pi)^{-1}$ is a geometric factor, and $\epsilon=4-d=1$ for dimension $d=3$. The Z functions are associated with their respective field-theoretic functions [4]

$$\zeta_r(u) = \mu\partial_\mu \ln Z_r(u,\epsilon)^{-1}|_0, \tag{13}$$

$$\zeta_\phi(u) = \mu\partial_\mu \ln Z_\phi(u,\epsilon)^{-1}|_0, \tag{14}$$

$$\beta_u(u) = u[-1 + \mu\partial_\mu (Z_u^{-1} Z_\phi^2)|_0] = -\left[\frac{d}{du}\ln(u Z_u Z_\phi^{-2})\right]^{-1}, \tag{15}$$

where the index 0 means differentiation at fixed r_0, ϕ_0, and u_0.

By introducing a flow parameter l, the effective coupling $u(l)$ satisfies the flow equation

$$l\frac{du(l)}{dl} = \beta_u(u(l)). \tag{16}$$

The flow parameter l is related to the correlation length by

$$\xi(l) = (\mu l)^{-1}. \tag{17}$$

The flow parameter value $l=0$ corresponds to the Ising fixed point $u(l=0)=u^*$, which is determined from $\beta_u(u^*)=0$. The

effective coupling $r(l)$ satisfies the flow equation

$$l\frac{dr(l)}{dl} = r(l)\zeta_r(u(l)). \tag{18}$$

The flow parameter value $l=1$ is an arbitrary reference point, at which the nonuniversal initial values are $u(l=1)\equiv u$ and $r(l=1)\equiv r=at$.

The values of the field-theoretic functions $\zeta_r(u)$, $\zeta_\phi(u)$, and $\beta_u(u)$ were calculated using the Borel resummations of five-loop expansions in the entire range $0<u<u^*$ [3,4]. Once the field-theoretic functions $\zeta_r(u)$, $\zeta_\phi(u)$, and $\beta_u(u)$ in Eqs. (13)–(15) are obtained, the reduced temperature, susceptibility, specific heat, and coexistence curve are given by [4,5]

$$|t| = \frac{\mu^2}{a} b_\pm(u(l))\exp\left[-\int_u^{u(l)} du' \frac{\zeta_r(u')-2}{\beta_u(u')}\right], \tag{19}$$

$$\chi_T^\pm = \frac{Z_\phi(u)}{\mu^2 f_\pm(u(l))}\exp\left[-\int_u^{u(l)} du' \frac{\zeta_\phi(u')+2}{\beta_u(u')}\right], \tag{20}$$

$$C_V^\pm = \frac{a^2 A_3 K_\pm(u(l))}{4\mu}\exp\left[-\int_u^{u(l)} du' \frac{1-2\zeta_r(u')}{\beta_u(u')}\right] + C_B, \tag{21}$$

$$\langle \Delta\rho_{L,V}\rangle^2 = \mu A_3 Z_\phi(u) f_\phi(u(l_-))\exp\left[-\int_u^{u(l_-)} du' \frac{\zeta_\phi(u')-1}{\beta_u(u')}\right]. \tag{22}$$

In Eqs. (19)–(22), $b_\pm$, $f_\pm$, $K_\pm$, and f_ϕ are the amplitude functions whose values at the fixed point u^* were calculated using the Borel resummations of five-loop expansions. Away from the fixed point, these amplitude functions were expanded to two-loop order at $u=0$ and additional extrapolation terms were added to reproduce the function values at the fixed point. All relevant references for the amplitude functions were given in Ref. [14]. $l_-=(\mu\xi_-)^{-1}$ is linked to the correlation length in coexisting phases. The quantity Z_ϕ is given by

$$Z_\phi(u)^{-1} = \exp\int_0^u du' \frac{\zeta_\phi(u')}{\beta_u(u')}. \tag{23}$$

The expressions, derived from Eqs. (19)–(22), for the leading and first Wegner expansion amplitudes of the three thermal properties are given in Ref. [14]. The correction-to-scaling exponent Δ is defined as $\Delta\equiv\nu\omega$ with $\omega = d\beta_u/du|_{u^*}$. The critical fluctuation background of specific heat, $B_{\rm cr}$, is implicitly contained in the first term of Eq. (21).

In general, the fit of a theoretical model to isothermal susceptibility, specific heat, and coexistence curve requires three system-dependent parameters, two for the determination of asymptotic amplitudes and one for the determination of the crossover. In the joint fit to the MSR model, these three system-dependent parameters correspond to μ, a, u. In addition, the analytical background for the specific heat C_B and the critical temperature T_c were also adjusted. Due to the strong nonlinearity in the MSR formulas, the fit would settle near any chosen initial value of u/u^* in the range $0.3<u/u^*<0.9997$. Scanned u/u^* in this range yielded a minimum in $\bar{\chi}_\nu^2$ at $u/u^* = 0.996\pm 6\times 10^{-10}$. Table I shows the covariance matrix generated from the joint fit. The off-diagonal elements represent the correlation between the fitting parameters. There is a strong correlation between μ and a in the MSR model when three model-specific fitting parameters were used. Hence the improvement in the minimization of $\bar{\chi}_\nu^2$ was insignificant compared to a two-parameter fit, using μ and a, previously performed in Ref.′ [14] on the same data set.

TABLE I. The covariance matrix generated from the joint fit of the MSR model to the experimental data. The off-diagonal elements represent the correlation between the fitting parameters.

	T_c	μ	a	u/u^*	C_B
T_c	1	0.28	0.29	0.22	0.13
μ	0.28	1	0.99	0.40	0.15
a	0.29	0.99	1	0.42	0.16
u/u^*	0.22	0.40	0.42	1	0.95
C_B	0.13	0.15	0.16	0.95	1

The MSR joint fit results are shown in Fig. 1 and compared with other models in Table VI. The Wegner expansions to first order are shown as dashed lines in Fig. 1 using the critical amplitudes, $\Gamma_0^\pm$ and $\Gamma_1^\pm$, $A_0^\pm$ and $A_1^\pm$, B_0 and B_1, calculated from the fit to the MSR ϕ^4 model.

IV. MASSIVE RENORMALIZATION SCHEME

Bagnuls and Bervillier (BB) developed a massive renormalization scheme [6,7] to describe critical behavior. In this field-theoretical framework, the Hamiltonian is the same as written in Eq. (8) except the bare coupling constant for the ϕ^4 term is $g_0/(4!)$ instead of u_0. The renormalization of the order parameter ϕ_0 and the bare parameters g_0 and a_0 are essentially the same as given in Eqs. (10)–(12).

BB derived the parametric expressions for their reduced temperature $\tau\equiv T/T_c-1$, correlation length, isothermal susceptibility, specific heat, and coexistence curve in terms of the renormalized coupling parameter g. This coupling parameter satisfied the flow equation (16) with the Wilson function $W(g)$ that is equivalent to the $\beta_u(u)$ function in the MSR analysis. For example, the expression for the isothermal susceptibility is given by $\chi_T=\chi_0\chi(g)$, where χ_0 is a fluid-dependent constant amplitude and $\chi(g)$ satisfies

$$\chi(g) = \chi(y_0)\exp\left[-\int_{y_0}^g dx \frac{\gamma(x)}{\nu(x)W(x)}\right]. \tag{24}$$

At the fixed point g^*, $\gamma(g^*)$ and $\nu(g^*)$ provide field-theoretical estimates of the critical exponents γ and ν. The functions of g for the reduced temperature, correlation length, isothermal susceptibility, specific heat, and coexistence curve were expanded in power series about $g=0$. The power series were then resumed over the entire range $]0,g^*[$.

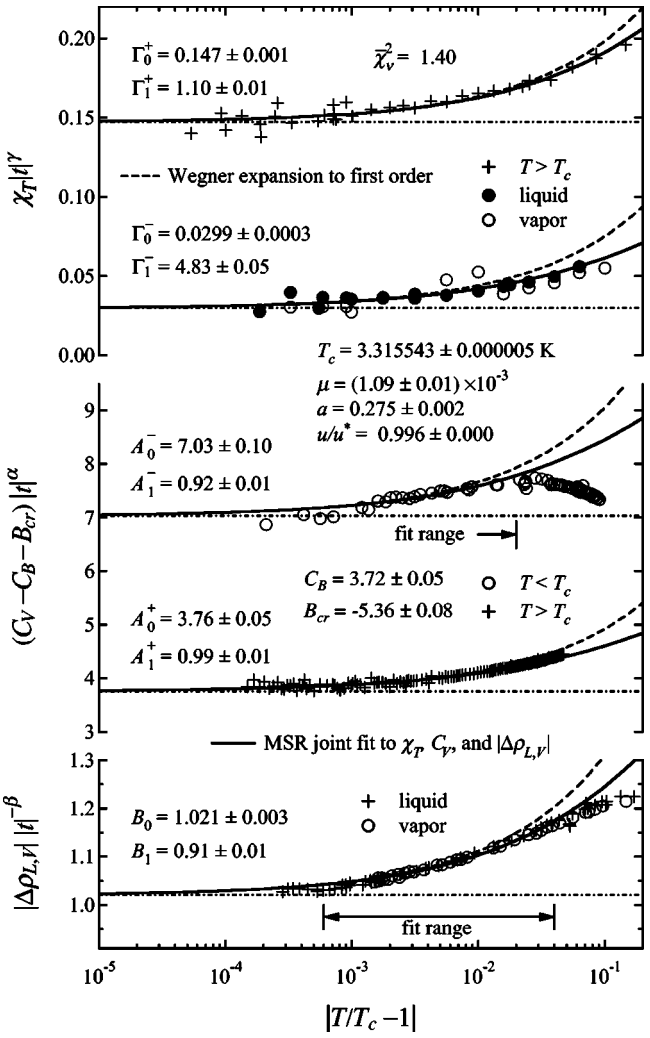

FIG. 1. A joint fit (solid lines) of the MSR model to the ^{3}He susceptibility, specific heat, and coexistence curve measurements. The fit used all the χ_T data and the C_V and $|\Delta\rho_{L,V}|$ data over the range indicated by the arrows. The dashed lines are the Wegner expansion to first order using the amplitudes calculated with the best fit parameters u/u^*, μ, and a. The values of the fitting parameters and calculated critical amplitudes are compared with other models in Table VI. The dot-dashed straight lines represent the asymptotic predictions from the fit.

Equation (24) can be transformed into an expression very similar to Eq. (20) using the scaling relation $\gamma = \nu(2-\eta)$ and the identity $\zeta_\phi(u^*) = -\eta$. Here η is the critical exponent of the fluctuation correlation at the critical point and ν is the critical exponent of the correlation length ξ. Thus the only difference between Eq. (24) and Eq. (20) is that the amplitude before the exponential function is a constant in Eq. (24) while it is a mild function of $u(l)$ in Eq. (20). Similar comparisons of the expressions for the specific heat and coexistence curve can be made between the MSR and MR schemes.

Recently Bagnuls and Bervillier reconsidered their MR scheme. They improved their sixth-loop series [10,11] and then made a new seventh-loop series [12]. In these sixth- and seventh-loop series, they chose a new convergence criterion for the Borel resummation of different functions like $\gamma(g)$ and $W(g)$ such that the "max" and "min" bounds of the resultant leading critical amplitude ratios agreed as closely as possible with the values obtained by Guida and Zinn-Justin [8]. Because of the "max" and "min" bounds on the Borel resummation, an envelope was obtained for each function such as $\chi(g)$. Two look-up tables were then made for a given property versus a temperature like scaling field t over the entire range $]0, g^*[$ for the "max" and "min" bounds. Bagnuls and Bervillier used the following empirical expression to fit the discrete data from a particular look-up table:

$$F(\tau) = Z\tau^\rho \prod_{i=1}^{N} (1 + X_i t^{D(t)})^{Y_i}, \tag{25}$$

$$D(t) = \Delta - 1 + \frac{S_1\sqrt{t}+1}{S_2\sqrt{t}+1}, \tag{26}$$

$$t = \theta|\tau|. \tag{27}$$

Here $N \leqslant 5$ depending on the required fit quality. In the homogeneous phase $T > T_c$, the $F(\tau)$ expression was used to calculate the correlation length inverse $\xi^{-1}(\tau)$, the susceptibility inverse $\chi_T^{-1}(\tau)$, and the specific heat $C_V(\tau)$. In the inhomogeneous phase $T < T_c$, the $F(\tau)$ expression was used to calculate the reduced liquid and vapor densities $\Delta\rho_{L,V}(\tau)$, the susceptibility inverse $\chi_T^{-1}(\tau)$ at the coexistence curve, and the specific heat $C_V(\tau)$ in the coexisting phases.

All the constants, Z, X_i, Y_i, and S_i, in Eqs. (25) and (26) are universal and are tabulated in Ref. [12]. For specific heat, another universal constant X_6 was added to $F(\tau)$ that is related to the critical fluctuation background. The universal asymptotic amplitude ratios were determined from the Z value in each $F(\tau)$. The proportionality factor θ is the link between t and the experimental reduced temperature τ. Here θ is a nonuniversal parameter that exclusively controls the magnitude of the corrections to scaling. The first Wegner amplitudes can be calculated using

$$\{\Gamma_1^\pm, A_1^\pm, B_1, \xi_1^\pm\} = K\theta^\Delta \sum_{i=1}^{N} X_i Y_i \tag{28}$$

with $K = -1$ for χ_T and ξ, and $K = +1$ for C_V and $\Delta\rho_{L,V}$.

Since there are two sets ("max" and "min") of $F(\tau)$ for each thermal property, their difference in the present theoretical calculation is generally much larger than the accuracy of the experimental measurements, sometimes neither one nor the other agreed with the measurements. To overcome this problem, Bagnuls and Bervillier defined a new theoretical function [12]

$$F_E(\tau) = [F_{\max}(\tau)]^E [F_{\min}(\tau)]^{1-E}, \tag{29}$$

with E being an additional adjustable parameter. In fitting $F_E(\tau)$ to experimental data, θ is an adjustable parameter for both $F_{\max}$ and $F_{\min}$. In the case of specific heat, a linearly mixed $X_6 = EX_6^{\max} + (1-E)X_6^{\min}$ term is added to F_E. When fitting to experimental data, $F_E(\tau)$ is scaled by a fluid-dependent amplitude (χ_0 for the isothermal susceptibility, c_0 for the specific heat, m_0 for the coexistence curve, and ξ_0 for

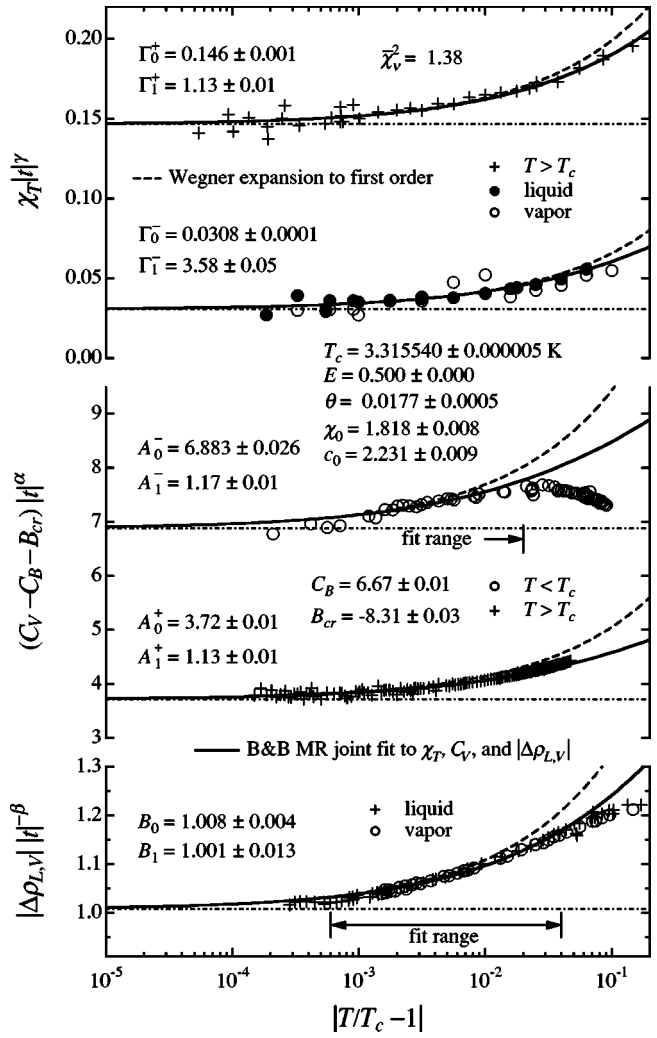

FIG. 2. A joint fit (solid lines) of BB's improved sixth-loop scheme to the ^{3}He susceptibility, specific heat, and coexistence curve measurements. The fit used all the χ_T data and the C_V and $|\Delta\rho_{L,V}|$ data over the range indicated by the arrows. The dashed lines are the Wegner expansion to first order using the amplitudes calculated with the best fit parameters χ_0, c_0, and θ. The values of the fitting parameters and calculated critical amplitudes are compared with other models in Table VI. The dot-dashed straight lines represent the asymptotic predictions from the fit.

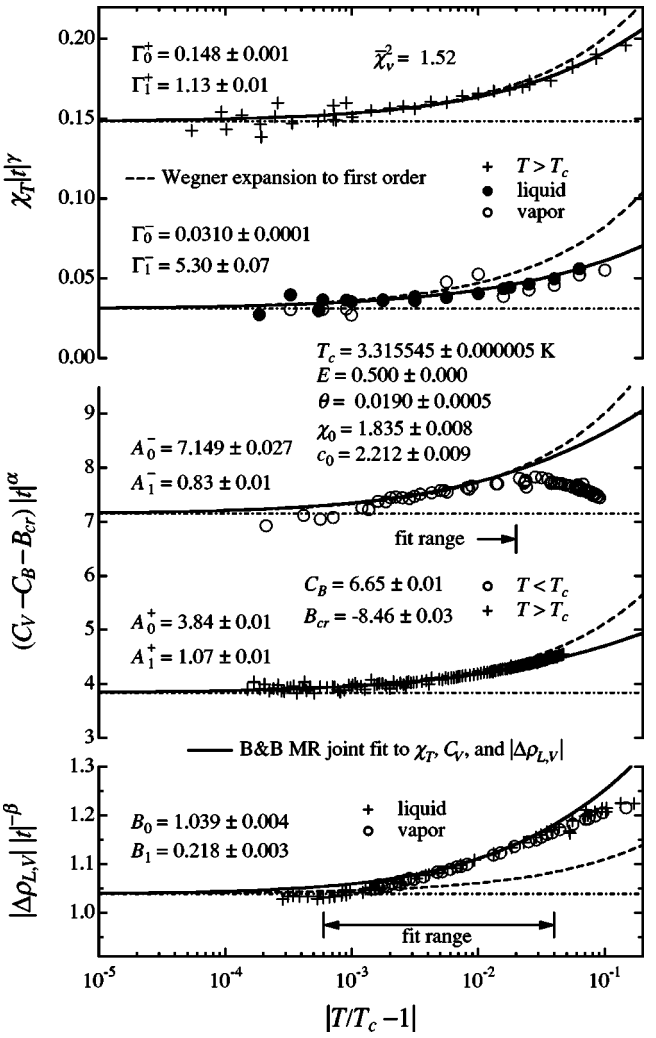

FIG. 3. A joint fit (solid lines) of BB's complete seventh-loop scheme to the ^{3}He susceptibility, specific heat, and coexistence curve. The fit used all the χ_T data and the C_V and $|\Delta\rho_{L,V}|$ data over the range indicated by the arrows. The dashed lines are the Wegner expansion to first order using the amplitudes calculated with the fitting parameters χ_0, c_0, and θ. The values of the best fit parameters and calculated critical amplitudes are compared with other models in Table VI. The dot-dashed straight lines represent the asymptotic predictions from the fit.

the correlation length). In our fit, χ_0 and c_0 were adjusted and m_0 was calculated through the universal ratio $R_c = \alpha A_0^+ \Gamma_0^+ / B_0^2$. E was initially fixed at 0.5 in order to have a minimum number of adjustable parameters when comparing the BB theory to other theoretical predictions.

Figure 2 shows the result of the joint fit of the experimental data to the improved sixth-loop predictions by Bagnuls and Bervillier [10,11]. Figure 3 shows the result of the joint fit of the same data to the new seventh-loop complete crossover predictions [12]. The weight and fitting ranges were the same as used for the MSR analysis. T_c and C_B were adjusted in addition to θ, χ_0, and c_0. The values of E fall outside valid range $0 \leqslant E \leqslant 1$ if it is allowed to vary in the fit. Table II shows the values of the goodness of fit for different fixed E values. On average, BB's improved sixth-loop scheme gave better fits than the seventh-loop scheme even though the seventh-loop scheme generated the smallest $\bar{\chi}_\nu^2$ with $E=1$.

The Wegner expansions to first order, calculated using the critical amplitudes $\Gamma_0^\pm$, $\Gamma_1^\pm$, $A_0^\pm$, $A_1^\pm$, B_0, and B_1 from the fit to the MR models, are also shown as dashed curves in Figs. 2 and 3. The dashed curves are consistently above the solid

TABLE II. The values of goodness of fit $\bar{\chi}_\nu^2$ for different mixing E values in the MR analysis.

E	Improved sixth loop	Complete crossover seventh loop
0.0	1.35	1.80
0.5	1.38	1.52
1.0	1.43	1.32

TABLE III. The covariance matrix generated from the joint fit of the MR sixth-loop scheme to the experimental data. The off-diagonal elements represent the correlation between the fitting parameters. The result from the seventh-loop scheme is almost identical.

	T_c	θ	χ_0	c_0	C_B
T_c	1	0.17	0.39	0.34	−0.07
θ	0.17	1	0.39	−0.02	−0.48
χ_0	0.39	0.39	1	0.90	0.05
c_0	0.34	−0.02	0.90	1	0.27
C_B	−0.07	−0.48	0.05	0.27	1

curves except for the coexistence curve from the seventh-loop analysis. When $E=1$ is used to minimize $\overline{\chi}^2_\nu$, the dashed curve of the Wegner expansion of the coexistence curve is above the solid curve.

Table III shows the correlation values of the MR fitting parameters. There is a strong correlation between the amplitude parameters χ_0 and c_0 that is similar to the correlation between μ and a found in the MSR analysis.

V. CROSSOVER PARAMETRIC EQUATION OF STATE

Agayan and Anisimov developed a new crossover parametric model equation of state [13] based on the original asymptotic extended parametric model [15]. In that model, the rescaled critical part of the classical local Helmholtz free-energy density is given by

$$\Delta\tilde{A}_{\rm cl} = \frac{1}{2}c_t\Delta\tilde{T}M^2 + \frac{u^*\overline{u}\Lambda}{4!}M^4 + \frac{1}{2}(\tilde{\nabla}M)^2. \tag{30}$$

Here the reduced temperature is defined as $\Delta\tilde{T}\equiv 1-T_c/T$ (which is different from the traditional definition of reduced temperature), $\overline{u}=u/u^*$ is a normalized coupling constant, Λ is a dimensionless cutoff wave number, and c_t characterizes the range of intermolecular interaction. In this scheme, u^* is the value of u at the fixed point of the Ising model, although its value is different from that of MSR because of different scaling in the Hamiltonian.

For a parametric equation of state in a reduced-temperature versus reduced-density plot, the radial variable r measures the distance to the critical point and angular variable θ measures the angle from the critical density and preserves the analytic dependence. Agayan and Anisimov formulated the crossover by rescaling the distance variable r with the crossover function Y that satisfied

$$1-(1-\overline{u})Y = \overline{u}[1+(\Lambda/\kappa)^2]^{1/2}Y^{\nu/\Delta}. \tag{31}$$

Here $\kappa^2=c_t r Y^{(2\nu-1)/\Delta}$ and ν is the critical exponent for the correlation length.

The scaling fields h_1, h_2, and the critical part of the thermodynamic potential $\Delta\tilde{\Phi}$ can be described by the parametric representation in terms of the variables r and θ as

$$h_1 = r^{3/2}Y^{(2\beta\delta-3)/2\Delta}\tilde{l}(\theta), \quad h_2 = rk(\theta), \tag{32}$$

and

$$\Delta\tilde{\Phi} = r^2Y^{-\alpha/\Delta}\tilde{w}(\theta) + \frac{1}{2}B_{\rm cr}r^2(1-b^2\theta^2)^2, \tag{33}$$

where the analytic functions of θ are

$$\tilde{l}(\theta) = \tilde{l}_0\theta(1-\theta^2), \quad k(\theta) = 1-b^2\theta^2, \tag{34}$$

$$\tilde{w}(\theta) = \tilde{m}_0\tilde{l}_0[w_0 + w_1\theta^2 + w_2\theta^4 + w_3\theta^6 + w_4\theta^8]. \tag{35}$$

Here $B_{\rm cr}=-2\tilde{m}_0\tilde{l}_0w_0<0$ is a fluctuation induced constant, $\tilde{m}_0=m_0g^{\beta-1/2}$, $\tilde{l}_0=l_0g^{\beta\delta-3/2}$, and $g=(\overline{u}\Lambda)^2/c_t$. The bare parameters m_0 and l_0 are two system-dependent coefficients that determine the asymptotic critical amplitudes. The two crossover parameters $\overline{u}$ and $\Lambda/c_t^{1/2}$ determine the shape of crossover and the crossover temperature scale [16]. The parameter b^2 and the coefficients $w_0\cdots w_4$ were selected such that all the universal asymptotic amplitude ratios were satisfied within their accuracies with the values given in the Ising model calculation of Ref. [17] while the ratios of the first correction-to-scaling amplitudes agreed within their accuracies with the values given by BB's earlier work [7].

In the lattice gas model, the ordering and nonordering fields h_1 and h_2 are mapped onto the physical fields of the chemical potential difference $\Delta\tilde{\mu}$ and reduced temperature $\Delta\tilde{T}$. Here $\Delta\tilde{\mu}\equiv(\rho_c/P_c)(T_c/T)(\mu-\mu_0)$ with $\mu_0(T)$ being an analytic function of temperature that is equal to the chemical potential μ when $h_1=0$.

For real fluids, the ordering and nonordering fields are approximated by linear combinations of the physical fields $\Delta\tilde{\mu}$ and $\Delta\tilde{T}$ in order to account for the corrections to scaling in the nonasymptotic regime. By choosing the value of the scaled energy density at the critical point to be $\tilde{u}_c=(\partial\tilde{P}/\partial\tilde{T})_{\tilde{\mu}}$ evaluated at the critical point, one can write the linear combination as

$$h_1 = \Delta\tilde{\mu}, \tag{36}$$

$$h_2 = \Delta\tilde{T} + b_2\Delta\tilde{\mu}, \tag{37}$$

with b_2 being the mixing parameter that is also a measure of the asymmetry in the slope of the coexistence curve. The parameters conjugate to the fields h_1 and h_2 are given by

$$\varphi_1 \equiv -\left(\frac{\partial\Delta\tilde{\Phi}}{\partial h_1}\right)_{h_2} = \Delta\rho - b_2\Delta\tilde{u}, \tag{38}$$

$$\varphi_2 \equiv -\left(\frac{\partial\Delta\tilde{\Phi}}{\partial h_2}\right)_{h_1} = \Delta\tilde{u}, \tag{39}$$

where $\Delta\rho\equiv(\rho/\rho_c-1)$ is the reduced fluid density and $\Delta\tilde{u}\equiv(\tilde{u}-\tilde{u}_c)$ is the difference between the scaled energy density and its value $\tilde{u}_c$ at the critical point.

To carry out the calculation further, the variables from h_1 and h_2 were changed to the parametric parameters r and θ. Once the analytic expressions for the first and second derivatives of r and θ with respect to h_1 and h_2 are obtained from the definition of h_1 and h_2 in Eq. (32) as functions of r and θ, the isothermal susceptibility, the specific heat at constant vol-

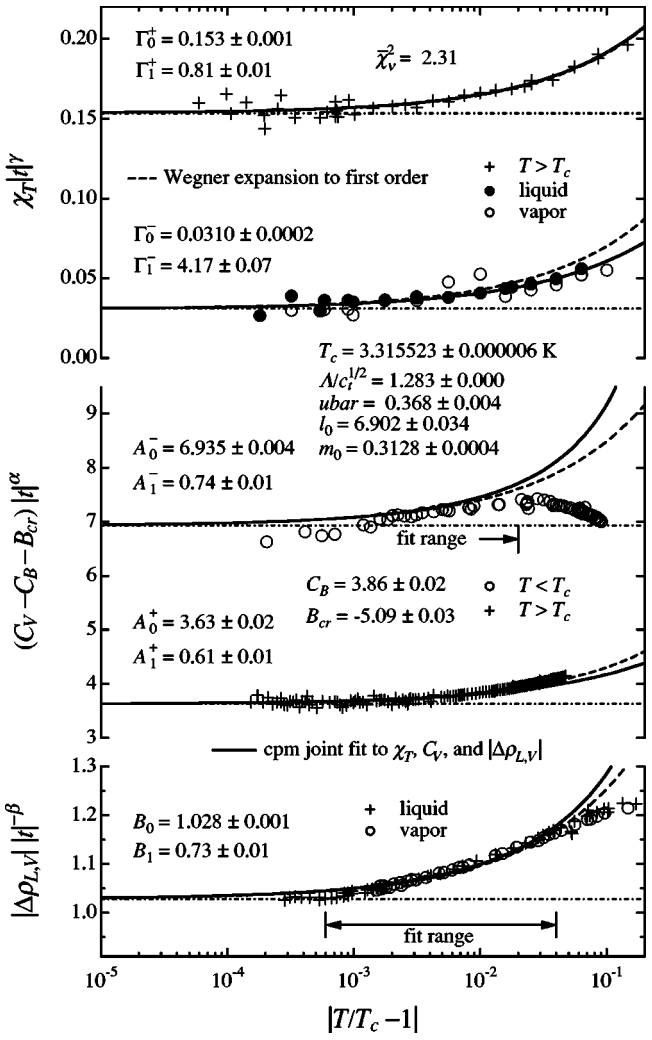

FIG. 4. A joint fit (solid lines) of the CPM model to the ^{3}He susceptibility, specific heat, and coexistence curve measurements. The fit used all the χ_T data and the C_V and $|\Delta\rho_{L,V}|$ data over the range indicated by the arrows. The dashed lines are the Wegner expansion to first order using the amplitudes calculated with the fitting parameters l_0, m_0, and $\bar{u}$. The values of the best fit parameters and calculated critical amplitudes are compared with other models in Table VI. The dot-dashed straight lines represent the asymptotic predictions from the fit.

ume, and the coexistence curve can be calculated from

$$\chi_T = \frac{T_c}{T}\left(\frac{\partial\rho}{\partial\tilde{\mu}}\right)_T, \tag{40}$$

$$C_V(T > T_c) = \left(\frac{T_c}{T}\right)^2\left(\frac{\partial\tilde{u}}{\partial\tilde{T}}\right)_\rho, \tag{41}$$

$$C_V(T < T_c, \rho = \rho_{\mathrm{cxc}}) = \left(\frac{T_c}{T}\right)^2\left(\frac{\partial\tilde{u}}{\partial h_2}\right)_{h_1}, \tag{42}$$

TABLE IV. The covariance matrix generated from the joint fit of the CPM model to the experimental data. The off-diagonal elements represent the correlation between the fitting parameters.

	T_c	$\bar{u}$	l_0	m_0	C_B
T_c	1	−0.15	0.37	−0.15	−0.18
$\bar{u}$	−0.15	1	−0.15	0.91	−0.50
χ_0	0.37	−0.15	1	−0.11	−0.49
c_0	−0.15	0.91	−0.11	1	−0.49
C_B	−0.18	−0.50	−0.49	−0.49	1

$$\Delta\rho_{L,V} = -\left(\frac{\partial\Delta\tilde{\Phi}}{\partial h_1}\right)_{h_2} - b_2\left(\frac{\partial\Delta\tilde{\Phi}}{\partial h_2}\right)_{h_1}. \tag{43}$$

For a specific heat measurement in the coexisting phases, the system follows the path of $\theta = \pm 1$ before and after a heat pulse is applied. From Eq. (32), it can be shown that $(\partial h_1/\partial\tilde{T})_{\theta=\pm1} = 0$, which implies $(\partial\tilde{u}/\partial\tilde{T})_{\theta=\pm1} = (\partial\tilde{u}/\partial h_2)_{h_1}(\theta = \pm 1)$. For a given reduced temperature and density, the parameters r and θ are solved numerically. It is well known that ^{3}He has the most symmetric coexistence curve among simple fluids. This implies that $b_2 \approx 0$ for ^{3}He. In this paper, we set $b_2 = 0$ to simplify our expressions and calculations. Along the critical isochore above T_c, one has $\theta = 0$ in the case $b_2 = 0$, thus $h_1 = 0$.

In the joint fit of the CPM model to the isothermal susceptibility, the specific heat, and the coexistence curve of ^{3}He, l_0, m_0, $\bar{u}$, C_B, and T_c were adjusted. In this fit, Λ is fixed at unity, the value obtained in the Ising model [18], and $c_t = 6/\pi^2$ is also fixed based on the approximation of the interaction range between fluid molecules [18]. The weighting and total standard deviation for each set of experimental data is the same as before. The joint fit results are shown in Fig. 4 and compared with other models in Table VI. The Wegner expansions to first order are also shown as dashed curves in Fig. 4 using the critical amplitudes $\Gamma_0^\pm$, $\Gamma_1^\pm$, $A_0^\pm$, $A_1^\pm$, B_0, B_1 calculated from the fit to the CPM model. These dashed curves are either above or below the solid curves that are calculated using the full CPM model. On the other hand, as shown in Figs. 1–3, the calculated Wegner expansion curves from the MSR and MR models are consistently above the solid curves calculated from the full models. The relatively large $\bar{\chi}_\nu^2$ generated from the fit to the CPM model appears to come from the large difference between theory and experiment in the specific heat below T_c.

Table IV shows the correlation values of the CPM fitting parameters. Again there is a strong correlation between two of the parameters $\bar{u}$ and m_0, similar to what was found in the MSR and MR analyses.

VI. UNIVERSAL AMPLITUDE RATIOS

Even though the leading amplitude and subsequent Wegner expansion coefficients are fluid dependent, certain combined ratios of these amplitudes are universal. From the equations for the first Wegner amplitudes of the specific heat,

TABLE V. The values of universal amplitude ratios obtained from various theoretical models.

Amplitude ratios	MSR[a]	MR(7)[b]	CPM[c]	FZ[d]
Γ_0^+/Γ_0^-	4.94	4.79±0.10	4.94	4.95±0.15
A_0^+/A_0^-	0.535	0.537±0.019	0.524	0.523±0.009
R_c	0.0580	0.0574±0.0020	0.0580	0.0581±0.0010
Γ_1^+/Γ_1^-	0.228	0.215±0.029	0.195	
A_1^+/A_1^-	1.07	1.36±0.47	0.83	
B_1/Γ_1^+	0.76	0.40±0.35	0.897	

[a]Zhong *et al.* [14].
[b]Bagnuls and Bervillier [12].
[c]Agayan and Anisimov [13].
[d]Fisher and Zinn [17].

susceptibility, coexistence curve, and correlation length, one notices in the MSR model that the system-dependent part is the same in every expression [14]. Equation (28) also shows that all first Wegner amplitudes share the same system-dependent θ^{Δ} in the MR scheme. Therefore the ratio of any of these first Wegner amplitudes is universal based on the MSR and MR ϕ^4 models. The expressions for these universal ratios in the MSR scheme have been given in Ref. [14]. In this paper we only list the values in Table V. The values given by Bagnuls and Bervillier are closely matched to those of Guida and Zinn-Justin [8] after the readjustment of the Borel resummation criteria [12].

VII. DISCUSSION

In this paper we have used parametric expressions to calculate the isothermal susceptibility, specific heat, and coexistence curve. These parametric expressions were based on the MSR, MR, and CPM theoretical models. All the critical leading amplitude ratios were defined in these models and their values are listed in Table V. The theories were fitted to the ^{3}He experimental data recently obtained for the isothermal susceptibility and specific heat, and earlier measurements of the coexistence curve. The agreement between these theories and experimental measurements is good.

TABLE VI. The dimensionless system-dependent parameters for ^{3}He. The adjustable parameters are obtained from the joint fit of the three different models to the measured χ_T, C_V, and $|\Delta\rho_{L,V}|$ data of ^{3}He. Zero uncertainty implies that the parameter is held constant during the fit.

	MSR	MR(6)[a]	MR(7)[b]	CPM
$\overline{\chi}_\nu^2$	1.40	1.38	1.52	2.31
	$u/u^*=0.996\pm0.000$	$E=0.5\pm0.0$	0.5±0.0	$\Lambda/c_t^{1/2}=1.283\pm0.000$
		$\theta=0.0177\pm0.0005$	0.0190±0.0005	$\overline{u}=0.368\pm0.004$
	$\mu\times10^3=1.09\pm0.01$	$\chi_0=1.818\pm0.008$	1.835±0.008	$l_0=6.902\pm0.034$
	$a=0.275\pm0.002$	$c_0=2.231\pm0.009$	2.212±0.009	$m_0=0.3128\pm0.0004$
C_B	3.72±0.05	6.67±0.01	6.65±0.01	3.86±0.02
T_c (fit)	3.315543±0.000005	3.315540±0.000005	3.315545±0.000005	3.315523±0.000006
Γ_0^+	0.147±0.001	0.146±0.001	0.147±0.001	0.153±0.001
Γ_0^-	0.0299±0.0002	0.0308±0.0001	0.0307±0.0001	0.0310±0.0002
Γ_1^+	1.10±0.01	1.13±0.01	1.17±0.01	0.81±0.01
Γ_1^-	4.83±0.05	3.58±0.05	5.49±0.05	4.17±0.07
A_0^+	3.76±0.05	3.72±0.01	3.80±0.02	3.63±0.02
A_0^-	7.03±0.09	6.88±0.03	7.09±0.03	6.935±0.004
A_1^+	0.99±0.01	1.13±0.01	1.10±0.01	0.61±0.01
A_1^-	0.92±0.01	1.17±0.01	0.86±0.01	0.74±0.01
B_{cr}	−5.39±0.08	−8.31±0.03	−8.38±0.03	−5.09±0.03
B_0	1.021±0.002	1.008±0.004	1.029±0.004	1.028±0.001
B_1	0.91±0.01	1.00±0.01	0.225±0.003	0.73±0.01

[a]Sixth-loop calculation.
[b]Seventh-loop calculation.

Although three model parameters were used in all the joint fits to the experimental data, the strong correlation observed between two of the three adjustable model parameters for each theoretical model suggests that ^{3}He as a simple fluid is situated very close to a renormalized trajectory that links the Gaussian and the Wilson-Fisher fixed points [19,20]. Because of this special feature of simple fluids, the roles played by other nonuniversal scales are effectively negligible, and the number of adjustable parameters can be reduced. The degree of degradation in the goodness of fit $\overline{\chi}_\nu^2$ due to the reduction of the adjustable parameters depends on the particular model. In the MSR case, the very high correlation of 0.99 between μ and a indicates that using only two adjustable parameters would not result in any significant decrease in the fit quality. The MSR model with one less adjustable parameter has a comparable $\overline{\chi}_\nu^2$ to that of the MR model. Both the MSR and MR models fit better than the CPM model which implies that they provide a better representation of the real fluid behavior near the critical point. The fitting parameters and the resultant critical amplitudes for all these models are listed in Table VI.

Although all the theoretical models tested in this paper provide a good description of experimental measurements along the critical isochore and coexistence curve, the more first-principle MSR and MR models are not complete equations of state. The CPM model is a complete equation of state even though it is phenomenological. This CPM model was developed to fit simple fluids as well as complex fluid systems that exhibit nonmonotonic crossover behavior. This nonmonotonic crossover behavior could be described by the CPM approach using a finite cutoff wavelength as an additional fitting parameter. However, in simple fluid systems like ^{3}He, crossover behavior of different physical quantities can be described quite well within the framework of the field theoretical ϕ^4 model without a finite cutoff wave number.

NASA has supported the development of future microgravity flight experiments [21,22] performing susceptibility, specific heat, and coexistence curve measurements of ^{3}He in the asymptotic region. Combining these possible future microgravity measurements in the asymptotic region with ground-based measurements in the crossover region would permit a rigorous test of the predictions of renormalization theories.

ACKNOWLEDGMENTS

We are grateful to Dr. Bervillier, Professor Anisimov, and Professor Dohm for a critical reading of the manuscript. The research described in this paper was carried out at the Jet Propulsion Laboratory, California Institute of Technology, under contract with the National Aeronautics and Space Administration.

[1] M. E. Fisher, in *Critical Phenomena*, edited by F. J. W. Hahne, Lecture Notes in Physics Vol. 186 (Springer, Berlin, 1982), p. 1.
[2] V. Dohm, Z. Phys. B: Condens. Matter **60**, 61 (1985).
[3] R. Schloms and V. Dohm, Europhys. Lett. **3**, 413 (1987).
[4] R. Schloms and V. Dohm, Nucl. Phys. B **328**, 639 (1989).
[5] R. Schloms and V. Dohm, Phys. Rev. B **42**, 6142 (1990).
[6] C. Bagnuls and C. Bervillier, Phys. Rev. B **32**, 7209 (1985).
[7] C. Bagnuls, C. Bervillier, D. Meiron, and B. Nickel, Phys. Rev. B **35**, 3585 (1987).
[8] R. Guida and J. Zinn-Justin, J. Phys. A **31**, 8103 (1998).
[9] S. A. Larin, M. Mönnigmann, M. Strösser, and V. Dohm, Phys. Rev. B **58**, 3394 (1998).
[10] C. Bagnuls and C. Bervillier, e-print hep-th/0112209.
[11] C. Bagnuls, C. Bervillier, D. I. Meiron, and B. G. Nickel, Phys. Rev. B **65**, 149901 (2002).
[12] C. Bagnuls and C. Bervillier, Phys. Rev. E **65**, 066132 (2002).
[13] V. Agayan, M. Anisimov, and J. Sengers, Phys. Rev. E **64**, 026125 (2001).
[14] F. Zhong, M. Barmatz, and I. Hahn, Phys. Rev. E **67**, 021106 (2003).
[15] M. E. Fisher, S.-Y. Zinn, and P. J. Upton, Phys. Rev. B **59**, 14533 (1999).
[16] M. A. Anisimov, S. Kiselev, J. V. Sengers, and S. Tang, Physica A **188**, 487 (1992).
[17] M. E. Fisher and S.-Y. Zinn, J. Phys. A **31**, L629 (1998).
[18] Y. Kim, M. Anisimov, J. Sengers, and E. Luijten, J. Stat. Phys. **110**, 591 (2003).
[19] C. Bagnuls and C. Bervillier, J. Phys. Stud. **1**, 366 (1997).
[20] C. Bagnuls and C. Bervillier, Condens. Matter Phys. **3**, 559 (2000).
[21] M. Barmatz, Report No. JPL-D17083, 2000 (unpublished).
[22] I. Hahn, Report No. JPL-D23024, 2002 (unpublished).